

62-51300  
JUN 24

GOVT. DOC.

Y3.N21/516/2095

NACA TN 2095

# NATIONAL ADVISORY COMMITTEE FOR AERONAUTICS

TECHNICAL NOTE 2095

APPLICATION OF THE WIRE-MESH PLOTTING DEVICE  
TO INCOMPRESSIBLE CASCADE FLOWS

By Willard R. Westphal and James C. Dunavant

Langley Aeronautical Laboratory  
Langley Air Force Base, Va.



Washington  
May 1950

CONN. STATE LIBRARY

BUSINESS, SCIENCE  
& TECHNOLOGY DEPT.

MAY 22 1950



TECHNICAL NOTE 2095

APPLICATION OF THE WIRE-MESH PLOTTING DEVICE  
TO INCOMPRESSIBLE CASCADE FLOWS

By Willard R. Westphal and James C. Dunavant

SUMMARY

The methods used in the application of the wire-mesh plotting device to find the flow pattern about a cascade of airfoils in incompressible inviscid flow and some mathematical checks that increase the accuracy of this application are described. Results for two typical turbine-blade cascades are shown to compare well with experimental data. A method of utilizing the wire mesh to design turbine blades with a prescribed pressure distribution in incompressible flow is presented.

INTRODUCTION

The analytical solution of the flow pattern existing about a cascade of airfoils in incompressible, nonviscous, two-dimensional flow is difficult and tedious.

Approximate solutions of the flow equations have been found by Weinig (reference 1) by sketching an orthogonal pattern of lines representing the streamlines and equipotential lines. By making a sufficient number of approximations, the resulting pattern can be made to correspond closely to the correct flow pattern for an ideal fluid. This process is very tedious and lacks accuracy.

On the wire-mesh plotting device developed by General Electric, (reference 2), the streamlines and equipotential lines are represented by a network of wires instead of by penciled lines. This device improves the accuracy and greatly reduces the time required to complete the flow pattern because small changes are easily made in the flow pattern.

A wire-mesh plotting device has been constructed at the Langley Aeronautical Laboratory and used successfully to find the flow pattern about turbine blade cascades. This paper describes the method used and presents a comparison of experimental two-dimensional cascade data and the data obtained by use of the wire-mesh plotting device. A method of finding the airfoil shape that will have a prescribed pressure distribution is also presented.

## SYMBOLS

c	chord
g	gap distance between corresponding points on adjacent blades
p	pressure
s	distance
x	distance along chord line
C	force coefficient $\left( \frac{2F}{\rho_1 V_1^2 c} \right)$
F	force on blade per unit span
M	mass flow
V	velocity
$\alpha$	angle between chord line and upstream velocity
$\beta$	stagger angle, angle between upstream velocity and normal to stagger line
$\Gamma$	circulation
$\epsilon$	angle between normal to stagger line (line tangent to leading edges of blades) and mean velocity
$\theta$	turning angle, angle between entering velocity and exiting velocity
$\rho$	density
$\sigma$	solidity $\left( \frac{c}{g} \right)$
$\phi$	potential function
Subscripts:	
1	upstream
2	downstream

a	perpendicular to stagger line, axial in a rotating machine
t	parallel to stagger line, tangential in a rotating machine
U	upper surface
L	lower surface
m	mean
n	normal to chord line
O	stagnation
T	total, resultant

#### TECHNIQUE OF PLOTTING FLOW THROUGH CASCADES

The wire-mesh plotting device used represented the stream and equipotential lines by 0.018-inch-diameter spring-steel wires. These lines must form curvilinear squares and cross each other at right angles at each intersection if they are to form a correct potential-flow pattern. They are made to cross at right angles by passing them through 0.020-inch-diameter holes drilled at right angles in a  $\frac{5}{32}$ -inch-diameter brass pin.

They are required to form squares by another network of wires placed at an angle of  $45^\circ$  with respect to the first network, and passing through another set of holes in the same pins (fig. 1). Lord Rayleigh (reference 3) has shown that if these diagonals intersect at right angles the stream and equipotential lines form curvilinear squares. Thus, the network tends to aline itself correctly if the boundary conditions are set; however, since the friction between the wires and pins is great enough to prevent free movement, the grid must be alined manually by making the wires intersect at right angles wherever they cross. The alinement of each square is facilitated by holding a small mirror against one of the streamlines, for example, perpendicular to the plot and observing the displacement of the image of the intersecting equipotential line from the equipotential line as viewed just over the top of the mirror (fig. 1). The mirror must be equipped with two short legs so that it can be used over the pins to check the angle between streamlines and equipotential lines.

In practice, the mesh is first alined as accurately as possible by eye and then the mirror is used to adjust each square individually. It is more convenient to start from the incoming flow and work downstream since the incoming flow direction and velocity are usually specified.

The potential-flow pattern to be obtained is for an infinite cascade; however, this can be represented with reasonable accuracy by plotting the flow through one passage between two successive blades and making the shape of the two stagnation streamlines the same. It is more convenient to work with two passages between three blades. The boundary streamlines are restrained by threading them through extra pins placed between the equipotential lines. The extra pins are held in place by  $\frac{3}{16}$ -inch-long  $\frac{1}{32}$ -inch-diameter sharpened pins projecting from their bottom surface.

As a first approximation for turbine-blade cascades, the position of the incoming stagnation streamline is assumed to be slightly below a line parallel to the entering velocity and perpendicular to the nose surface. The accuracy of this assumption will become evident as the incoming flow field is alined from it. If the stagnation streamline has been properly assumed, the stagnation streamlines of adjacent blades will have the same shape. If all the incoming stagnation streamlines are not the same, their positions must be changed and the plot realined. This process is repeated until they are the same when the plot is alined. If the flow plot is correct, the two passages plotted will have the same flow patterns. It should also be noted that the number of potential lines between nose stagnation points is equal to the number of squares per passage of cascade times the tangent of  $\beta$ . Near the leading-edge stagnation point the velocity is changing rapidly; therefore, each of the adjacent squares of the network represents an average of a wide range of velocities and is not as nearly perfect a square as the other squares so that the determination of the position of the stagnation point is more difficult. Therefore, the velocity distribution near the nose does not show small local velocity peaks unless the area of the high-velocity region is of the same order of magnitude as the squares of the network. For this reason, a network consisting of a large number of small squares is desirable. However, such a network requires more time to aline than one with fewer squares so a compromise must be made. For turbine cascades, five squares per passage of the cascade has been found to give satisfactory results. With such a network, a solution was obtained in 30 hours; however, with practice, the time needed for this type of plot has been reduced to 16 hours. The airfoils should be large enough so that the smallest square is about  $\frac{3}{4}$  inch long.

For a compressor cascade with a solidity of 1.5 and a stagger angle of  $45^\circ$ , a grid having 10 squares per passage of cascade has failed to give satisfactory results largely because of the difficulty in determining the position of the stagnation streamline. The position of the nose streamline must be determined more accurately for compressor blades than for turbine blades because the entering velocity is higher and the turning angle and circulation are lower. The lower solidity and turning

angle of compressor cascades combine to produce a passage that is less well defined than a typical turbine-blade passage.

For turbine blades having guidance (a straight portion at the trailing edge), the exit flow may be assumed to be parallel to the mean line at the trailing edge of the blades. The two trailing-edge streamlines are brought together insofar as this is mechanically possible.

#### CHECKS ON ACCURACY OF PLOT

When the wire-mesh plotting device is used to find the flow pattern about airfoils in cascade, the mechanical accuracy of the plot may be checked by comparing the forces exerted on the blade as calculated from three different sets of data obtained from the plotting device. The normal-force coefficient  $C_n$  can be found from the change of momentum and pressure as calculated from the velocity diagram, from the measured circulation, and from the integrated area of the pressure distribution.

If the plot is correct, these three values of the force will be equal. If they are not equal, the plot must be readjusted until agreement is reached. Weinig presents these checks on accuracy as they apply to graphical solutions obtained by sketching (reference 1).

The force coefficient can be found from the velocity diagram as the vector sum of the components perpendicular and parallel to the stagger line. The force perpendicular to the stagger line consists of a pressure force only. For each blade, figure 2,

$$F_a = (p_1 - p_2)g$$

therefore

$$F_a = \frac{\rho_1}{2}(V_2^2 - V_1^2)g$$

or, in coefficient form,

$$C_a = \frac{V_2^2 - V_1^2}{\sigma V_1^2}$$

The force parallel to the stagger line is due to the momentum change only since the pressures along two similar streamlines (such as AB and CD in fig. 2) are equal and opposite, that is,

$$F_t = M \Delta V_t$$

where for one blade passage:

$$\begin{aligned} M &= g\rho_1 V a_1 \\ &= g\rho_1 V_1 \cos \beta \end{aligned}$$

and

$$\Delta V_t = V_{t_1} - V_{t_2}$$

Therefore

$$F_t = g\rho_1 V_1 \cos \beta (V_{t_1} - V_{t_2})$$

or, in coefficient form,

$$C_t = \frac{2 \cos \beta}{V_1 \sigma} (V_{t_1} - V_{t_2})$$

From figure 3, the component of the force coefficient normal to the chord line equals

$$C_n = C_a \sin(\alpha - \beta) + C_t \cos(\alpha - \beta)$$

The second value of  $C_n$  is found from the measured value of the circulation. It can be shown (reference 1) that the total force on an airfoil in cascade is equal to

$$F_T = \rho V_m \Gamma$$



where

$V_m$  vector mean of entering and exiting velocities

$\Gamma$  circulation

This force acts perpendicular to the mean velocity.

By definition:

$$\Gamma = \oint V ds$$

taken completely around the airfoil and

$$\varphi = \oint V ds$$

along any path; therefore,

$$\Gamma = \Delta\varphi_U - \Delta\varphi_L$$

where

$\Delta\varphi$  number of squares between stagnation points along the surface divided by the number of squares in unit distance at unit velocity

$\Delta\varphi_U, \Delta\varphi_L$  increase in potential from leading to trailing stagnation points along the upper and lower surfaces, respectively

Therefore,

$$F_T = \rho V_m (\Delta\varphi_U - \Delta\varphi_L)$$

or, in coefficient form,

$$C_T = \frac{2V_m(\Delta\varphi_U - \Delta\varphi_L)}{V_1^2 c}$$

From figure 3, the component of the total-force coefficient that acts normal to the chord is seen to be

$$C_n = C_T \cos(\alpha - \beta + \epsilon)$$

From figure 4,

$$\epsilon = \tan^{-1} \frac{V_{t1} + V_{t2}}{2V_1 \cos \beta}$$

The third value of  $C_n$  can be found from integrating the pressure distribution around the blade as follows:

$$F_n = \int_0^c (P_L - P_U) dx$$

but

$$P_L = P_0 - \frac{1}{2} \rho V_L^2$$

and

$$P_U = P_0 - \frac{1}{2} \rho V_U^2$$

Therefore

$$F_n = \frac{\rho}{2} \int_0^c (V_U^2 - V_L^2) dx$$

and

$$C_n = \int_0^c \left[ \left( \frac{V_U}{V_1} \right)^2 - \left( \frac{V_L}{V_1} \right)^2 \right] \frac{dx}{c}$$

Since  $V = \frac{\Delta p}{\Delta s}$  at any point and  $\Delta p$  is a constant increment between adjacent wires,

$$\left(\frac{V_L}{V_1}\right)^2 = \left(\frac{ds_1}{ds_L}\right)^2$$

and

$$\left(\frac{V_U}{V_1}\right)^2 = \left(\frac{ds_1}{ds_U}\right)^2$$

In practice, the increment  $\Delta s$  is measured between adjacent wires along the blade and the corresponding velocity is assumed to occur on the surface midway between the wires.

#### COMPARISON WITH CASCADE-TUNNEL DATA

An example of the solution to the direct problem is shown in figure 5, which is the completed flow pattern about a reaction turbine blade, blade I, at a stagger angle of  $30^\circ$  and a solidity of 1.8. The position of the leading-edge stagnation streamline was assumed and the grid was then alined from the leading edge rearward, the leading-edge stagnation streamline being changed as necessary.

The alining process was repeated until the following three approximately equal values of  $C_n$  were obtained:

Source	$C_n$
Velocity diagram	1.280
Circulation	1.294
Pressure distribution	1.272

After the flow plot was made, the blade shape was tested in a 20-inch cascade tunnel at Langley using seven, 6-inch-chord blades. The center blade was fitted with pressure orifices along the upper and lower surfaces at the midspan to obtain a pressure distribution.

The pressure distributions from the flow plot and cascade-tunnel tests are compared in figure 6. The angles measured were as follows:

Source	$\beta$ (deg)	$\alpha$ (deg)	$\theta$ (deg)
Flow plot	30	53.4	74
Cascade	31	54.4	73.3

Another example of the direct problem is shown in figure 7, the flow pattern about a reaction turbine blade, blade II, at  $30^\circ$  stagger and a solidity of 1.8. The pressure distributions compared well (fig. 8) and, although the cascade-tunnel stagger angle, angle of attack, and turning angle differed from those of the flow plot by approximately  $2^\circ$  because of a  $2^\circ$  upstream tunnel flow angle, the leaving-air angle was only  $0.2^\circ$  larger than that predicted by the flow plot:

Source	$\beta$ (deg)	$\alpha$ (deg)	$\theta$ (deg)
Flow plot	30.0	59.2	86
Cascade tunnel	32.0	61.8	88.2
Difference	2.0	2.6	2.2

The integrated area of the cascade-tunnel pressure distribution was slightly greater than that of the flow plot. This result is consistent with the greater turning angle measured in the tunnel.

This method of flow plotting has been applied to two other turbine cascades, one at  $45^\circ$  stagger and one at  $30^\circ$  stagger. The data obtained have compared as well with cascade data as the numerical examples given above. On the basis of these results, it appears that this method is sufficiently accurate to replace low-speed cascade tunnels in the preliminary design and evaluation of turbine-blade profiles.

#### THE INVERSE PROBLEM

The inverse problem, that of finding the blade shape when the pressure distribution, turning angle, stagger, and solidity are prescribed, was attempted for an impulse blade, blade III, at  $45^\circ$  stagger,  $90^\circ$  turning, and a solidity of 1.8. The pressure distributions along the

upper and lower surfaces were prescribed as having constant values of  $(V/V_1)^2$  over the first 60 percent of the chord of 1.9 and 0.5, respectively. The pressure distribution over the last 40 percent chord was not prescribed. The stagger, and hence  $\Delta s_1$ , being known,  $\Delta s_U$  and  $\Delta s_L$  were calculated and the lengths of these increments set on the grid by small metal links joining the pins. The alinement of this setup, however, was a problem too difficult for solution and in order to allow more freedom of movement the links were removed from the lower surface since the velocities there are of less interest. The plot was then alined from the entering flow rearward, a pressure distribution over the lower surface being selected so that the upper and lower surfaces intersected at a specified chord and gave the desired turning angle. With this simplification, an experienced operator obtained the blade shape in approximately 32 hours. The completed flow plot is shown in figure 9.

In the cascade-tunnel test of the resulting blade section, the pressure distribution (fig. 10) showed a velocity peak which was not indicated by the flow-plotting device. This discrepancy was attributed to the mechanical difficulty of shaping and alining the wires at the leading edge, a condition made worse by the interference of the metal links with the mirror, and the inherent inaccuracies of the flow plot near the stagnation point. The nose of the blade shape was modified by cutting it to an NACA 64<sub>2</sub>-015 airfoil nose shape which extended to about 12 percent chord. After modification, the shape was retested in a cascade tunnel and on the plotting device by the direct method. The pressure distributions obtained are shown in figure 11. Satisfactory agreement was obtained.

For the inverse method, in order to avoid velocity peaks on the nose, it is therefore better to start with a known nose shape laid out to 10 percent chord and plot the surfaces rearward from it.

### CONCLUSIONS

A wire-mesh plotting device has been used to find the flow pattern about four turbine cascades at stagger angles of 30° and 45° and a solidity of 1.8, and one compressor cascade at a stagger angle of 45° and a solidity of 1.5. One turbine profile was determined by an inversion of the method. The accuracy of these plots has been improved by equating the lift as calculated by three different methods and using a mirror to check the orthogonality of each square as a further check on the mechanical accuracy of the plot. From a comparison of plotting-device data with cascade-tunnel data for these cases, it may be concluded that:

1. A wire-mesh plotting device may be used to find the turning angle and pressure distribution about a given turbine-blade cascade in two-dimensional incompressible flow. Data sufficiently accurate to replace low-speed cascade-tunnel testing in the preliminary design and evaluation of turbine-blade shapes may be obtained.

2. The inverse problem of finding a turbine-blade shape that will have a prescribed turning and pressure distribution over the upper surface may also be solved by the use of this plotting device. It is advisable to use a known shape for the first 10 percent of the blade as the plotting device is not accurate near the stagnation point.

3. Compressor-blade cascade problems are not easily solved by this method because of the difficulty of accurately positioning the stagnation streamlines.

Langley Aeronautical Laboratory  
National Advisory Committee for Aeronautics  
Langley Air Force Base, Va., March 13, 1950

## REFERENCES

1. Weinig, F: Die Strömung um die Schaufeln von Turbomaschinen. Johann Ambrosius Barth (Leipzig), 1935.
2. Poritsky, H., Sells, B., and Danforth, C. E.: Graphical, Mechanical and Electrical Aids for Compressible Fluid Flow. Data Folder 46150, Aircraft Gas Turbine Eng. Div., Gen. Elec. Co., Aug. 13, 1948.
3. Rayleigh, (Lord): On the Dynamics of a Revolving Fluid. Scientific Papers, vol. VI, Cambridge Univ. Press, 1916.

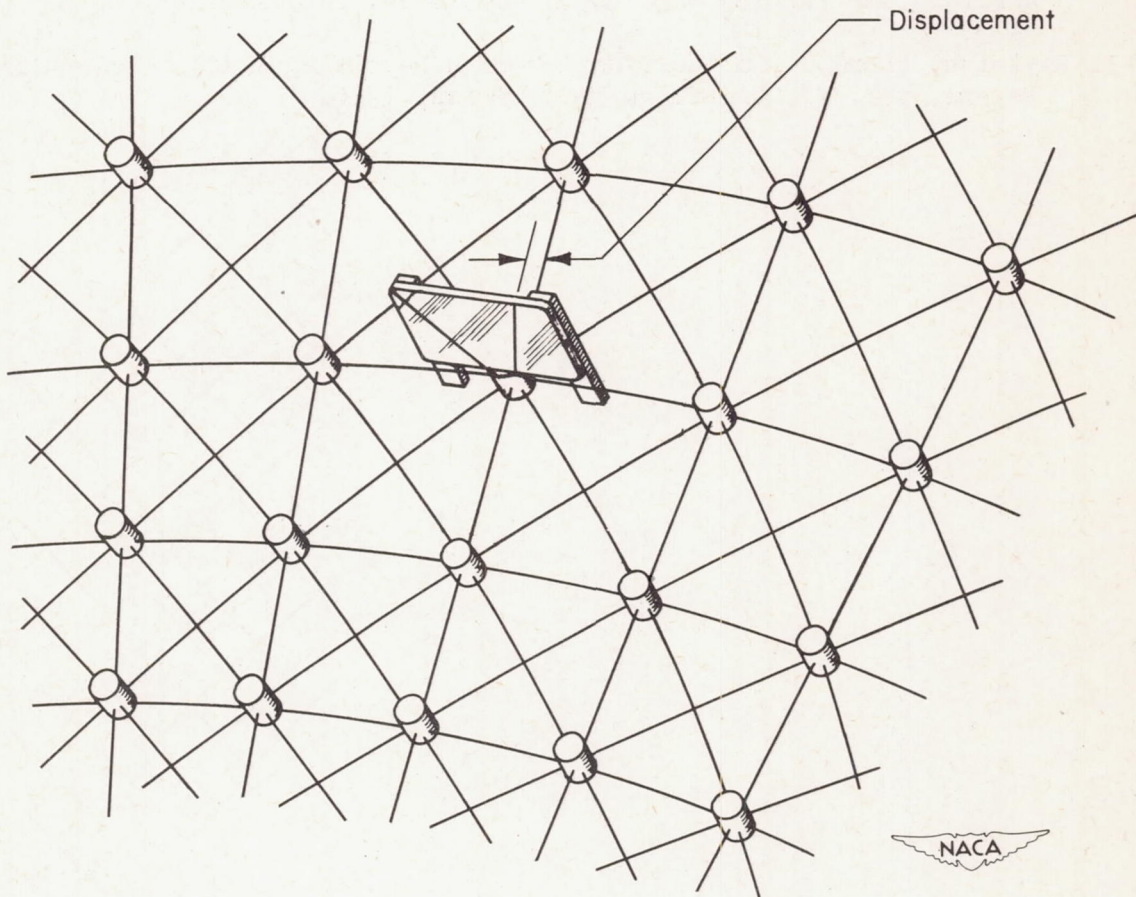
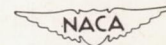


Figure 1.- Wire-mesh alinement.





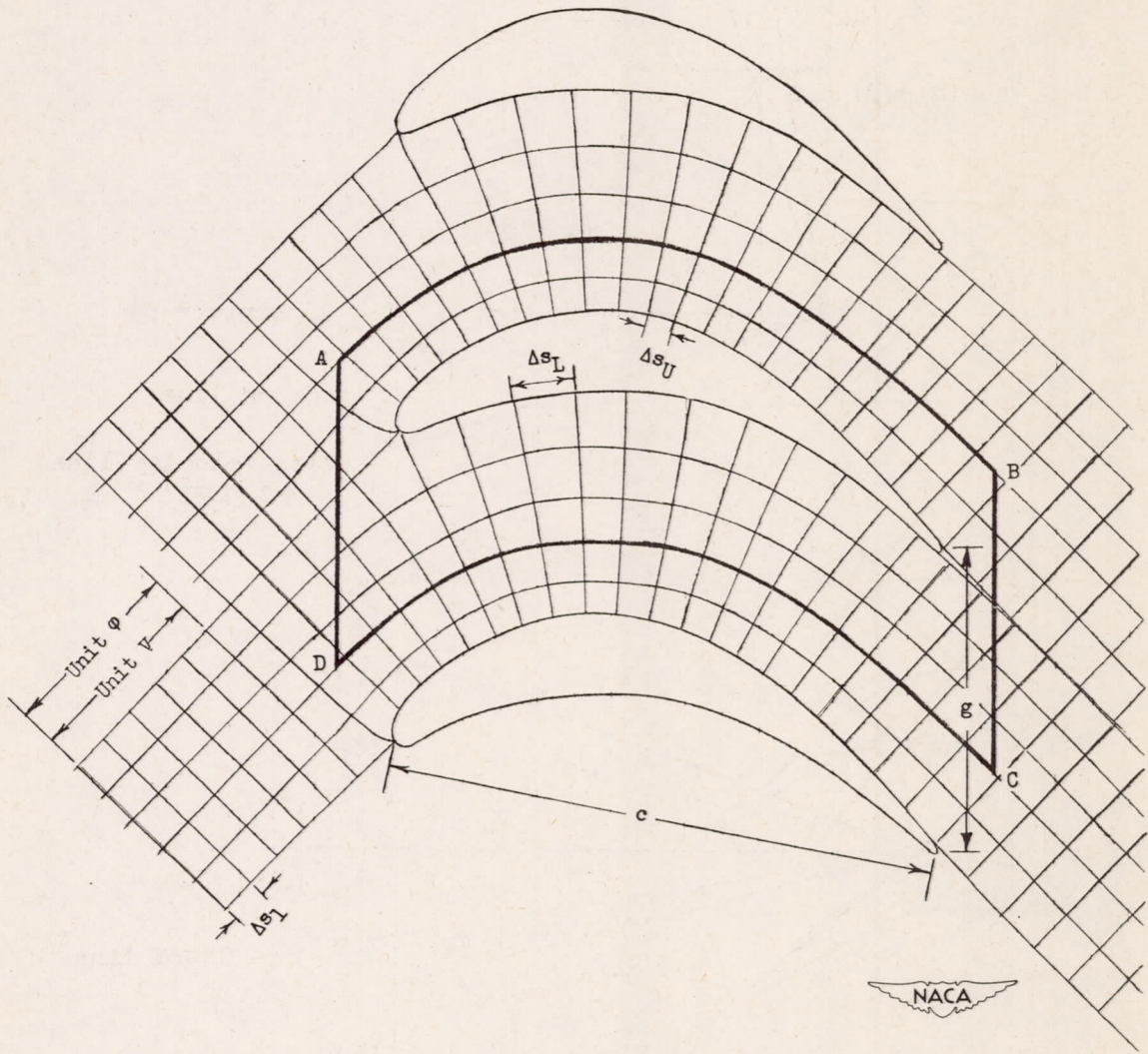


Figure 2.- Flow pattern.

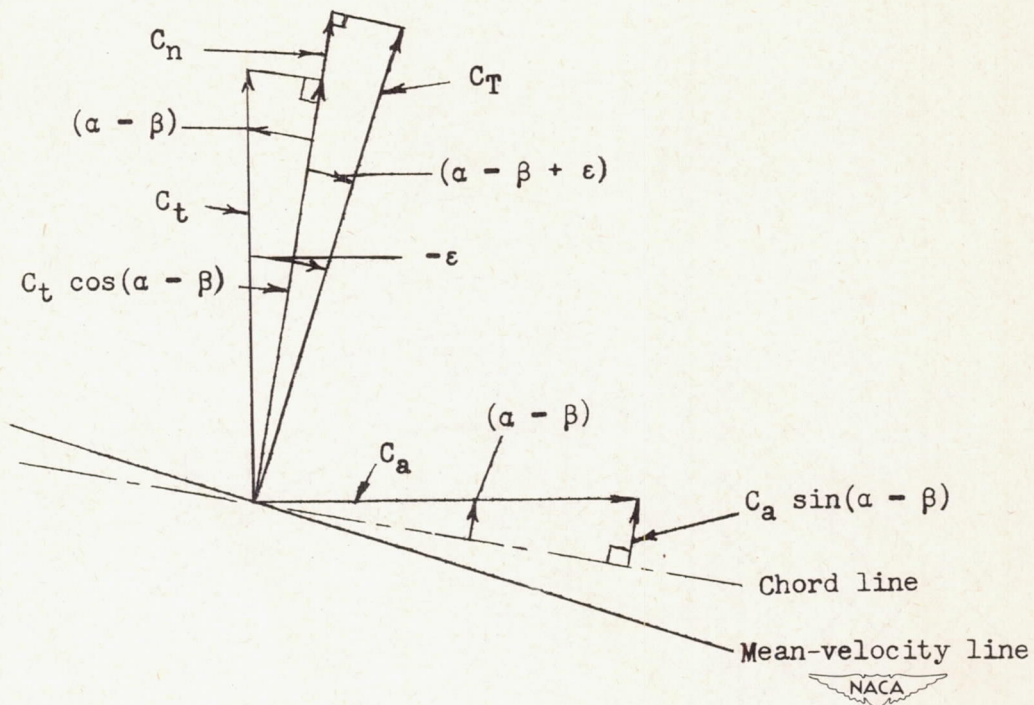


Figure 3.- Force diagram.

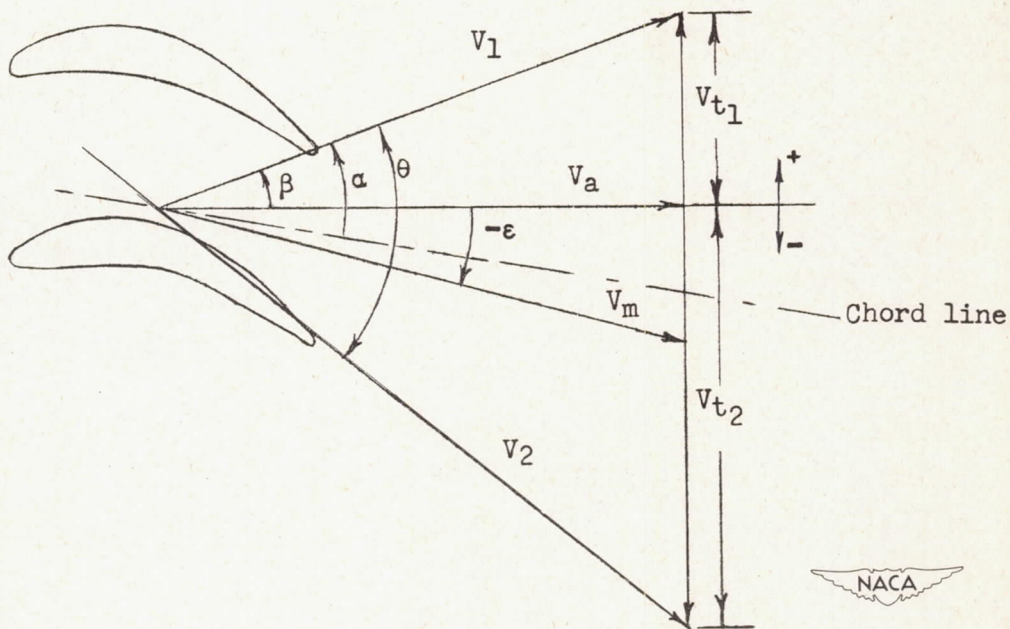


Figure 4.- Velocity diagram.

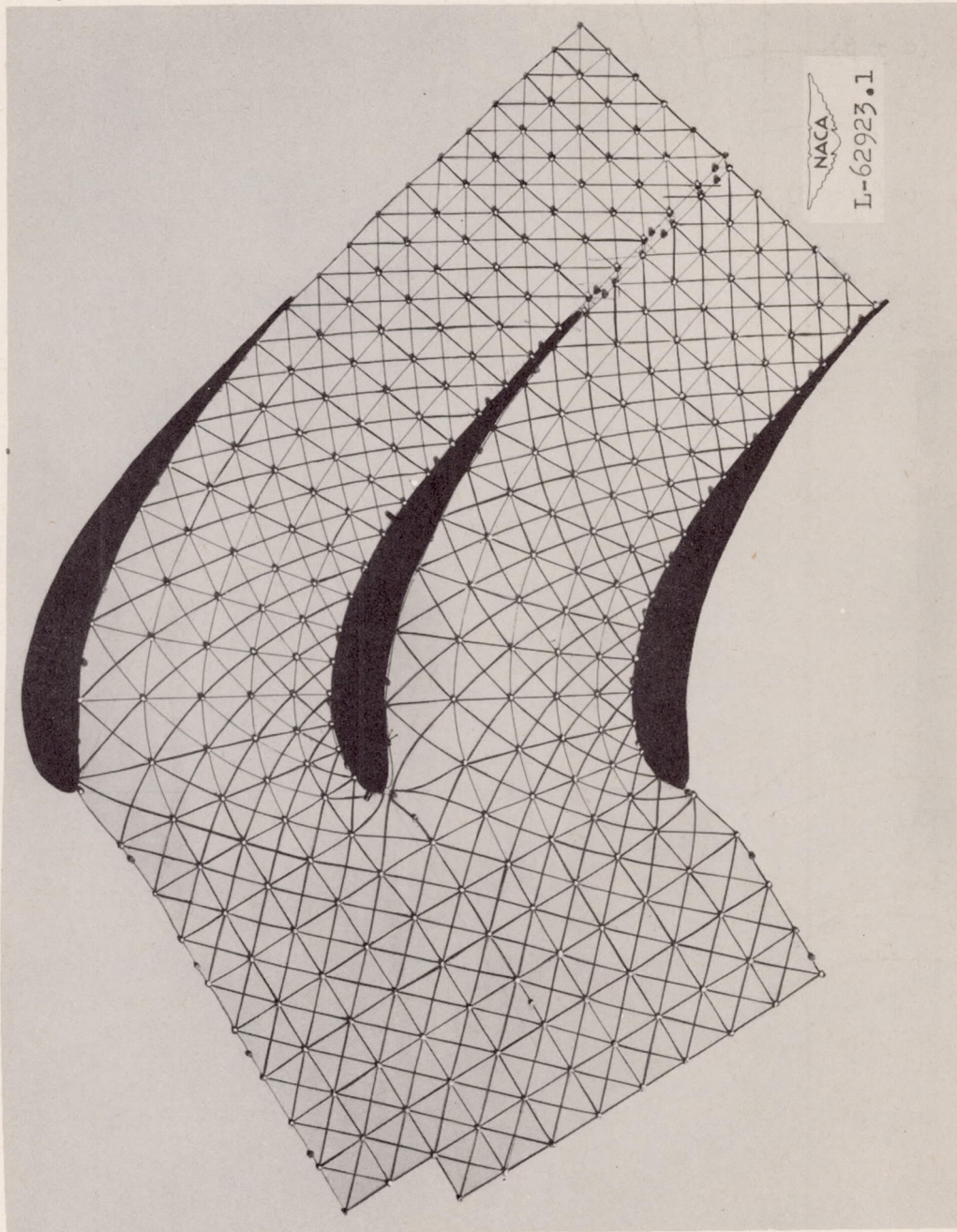


Figure 5.- Flow pattern for blade I.



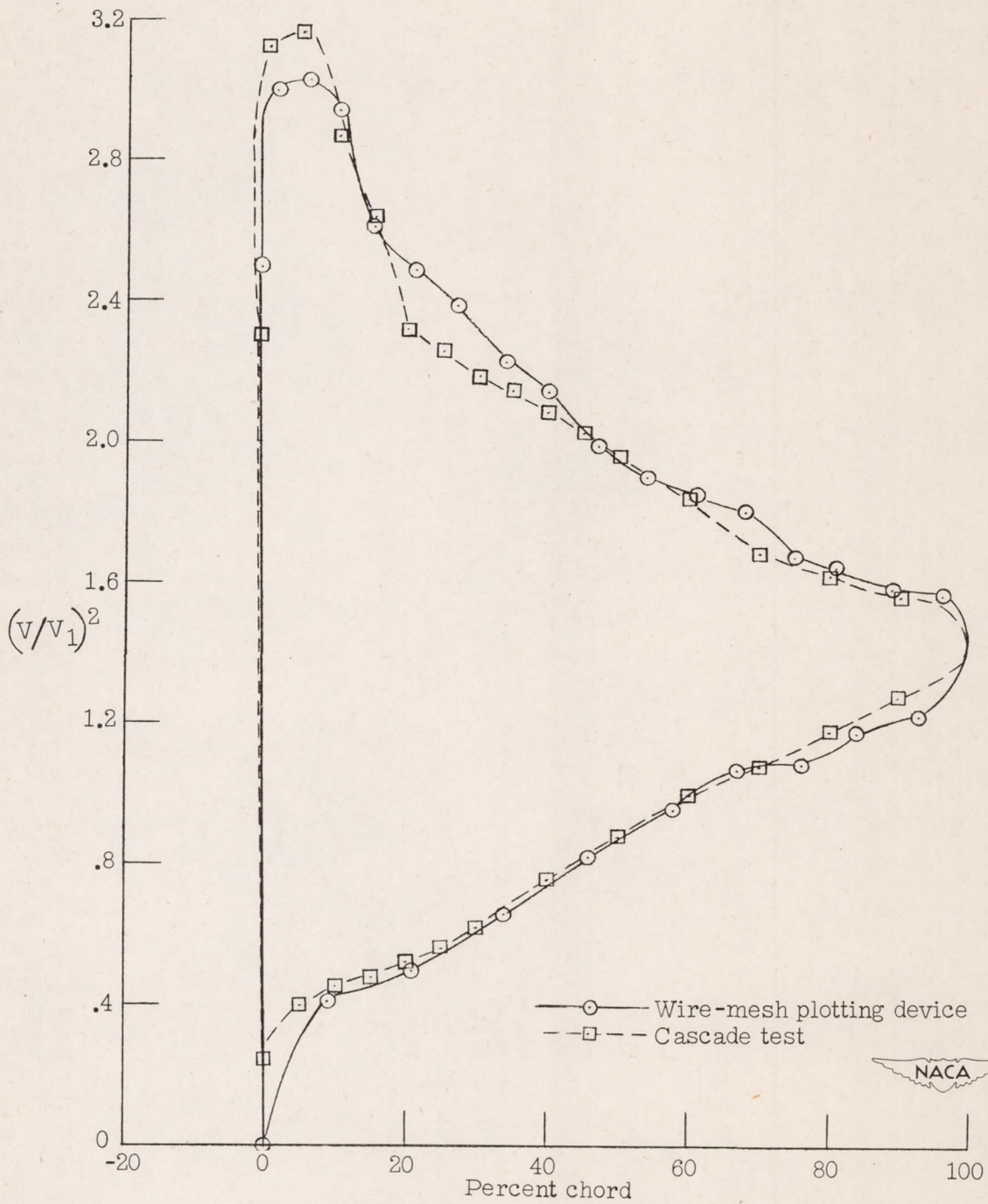
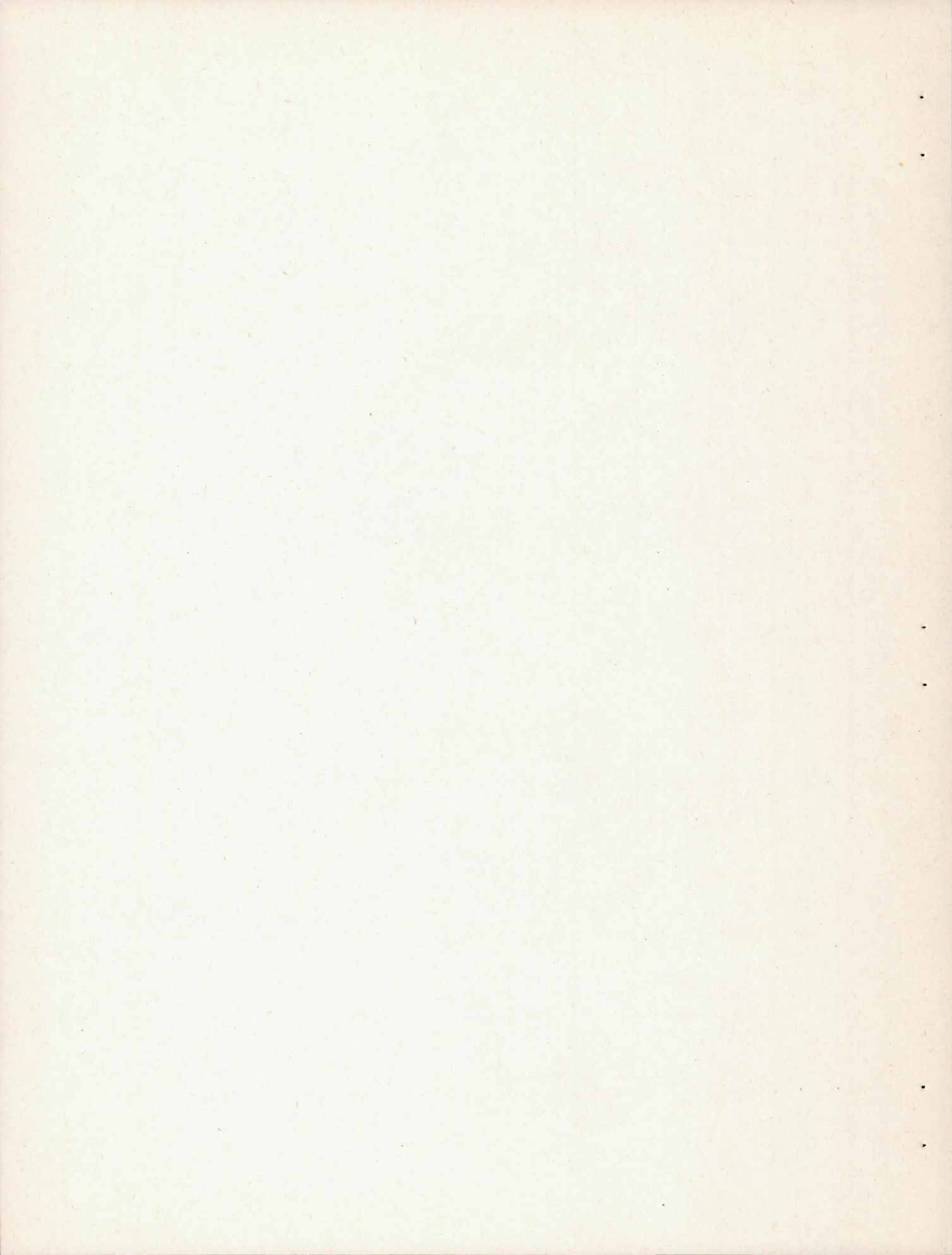


Figure 6.- Pressure distribution for blade I at 30° stagger and 1.8 solidity.



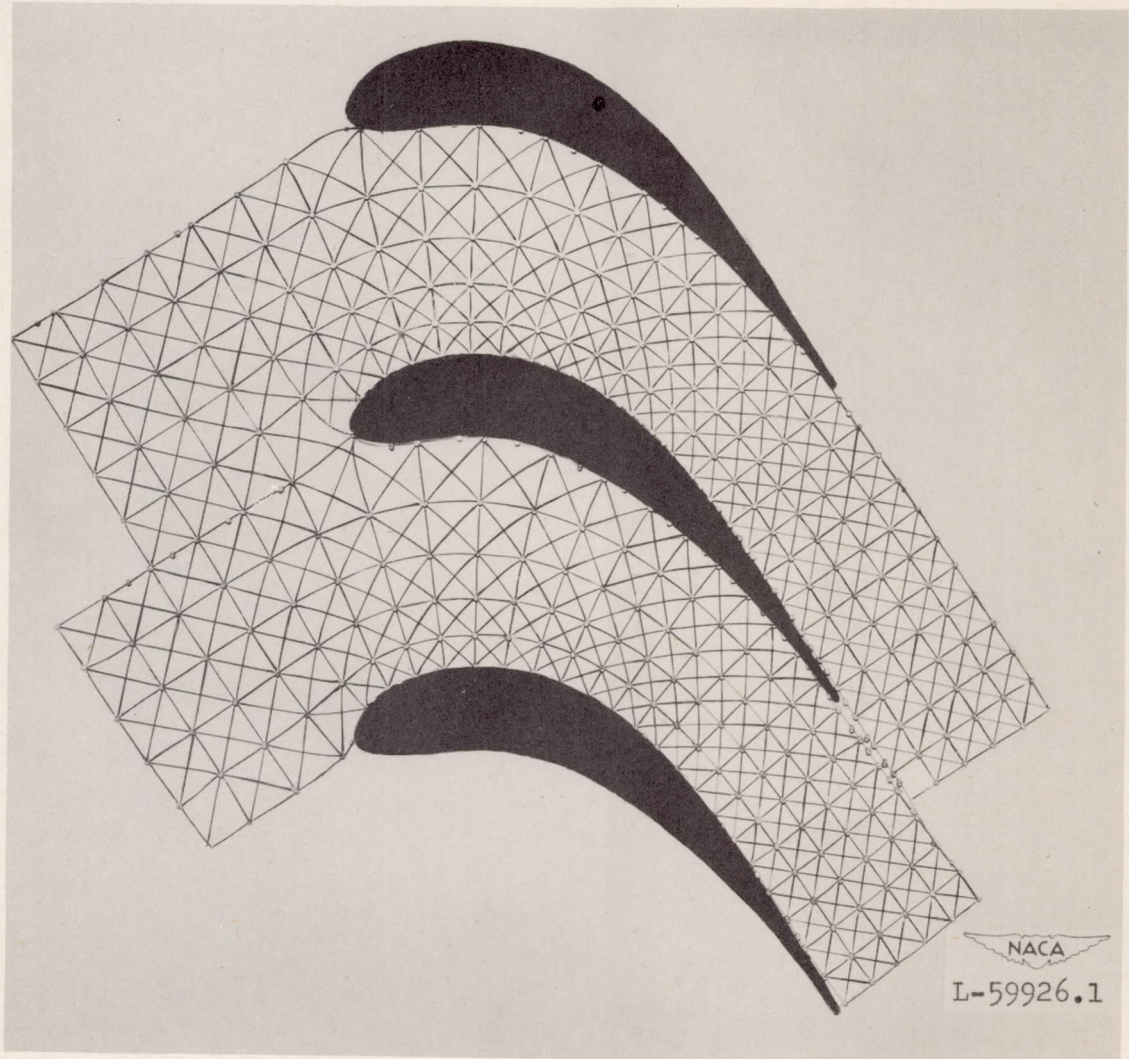
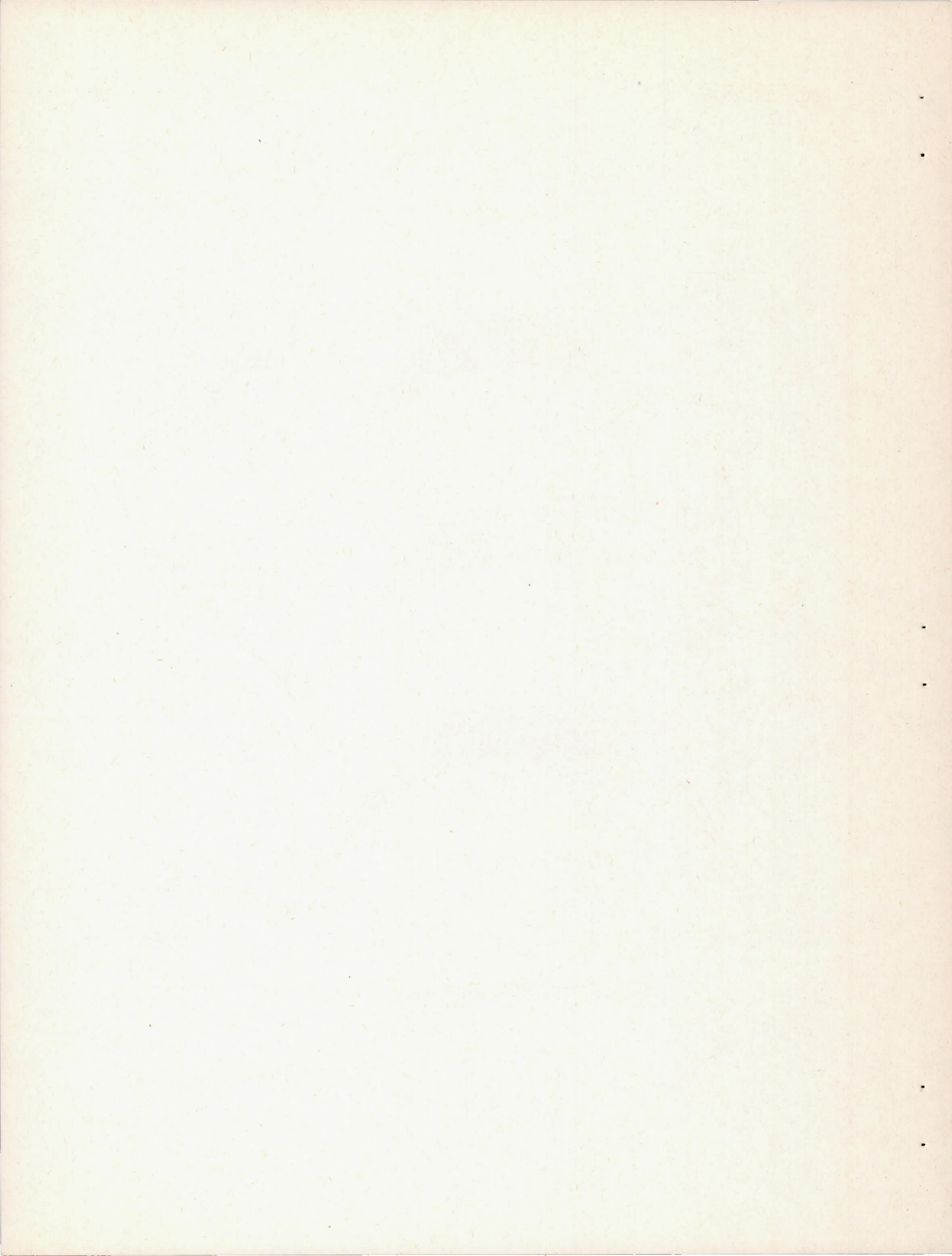


Figure 7.- Flow pattern for blade II.





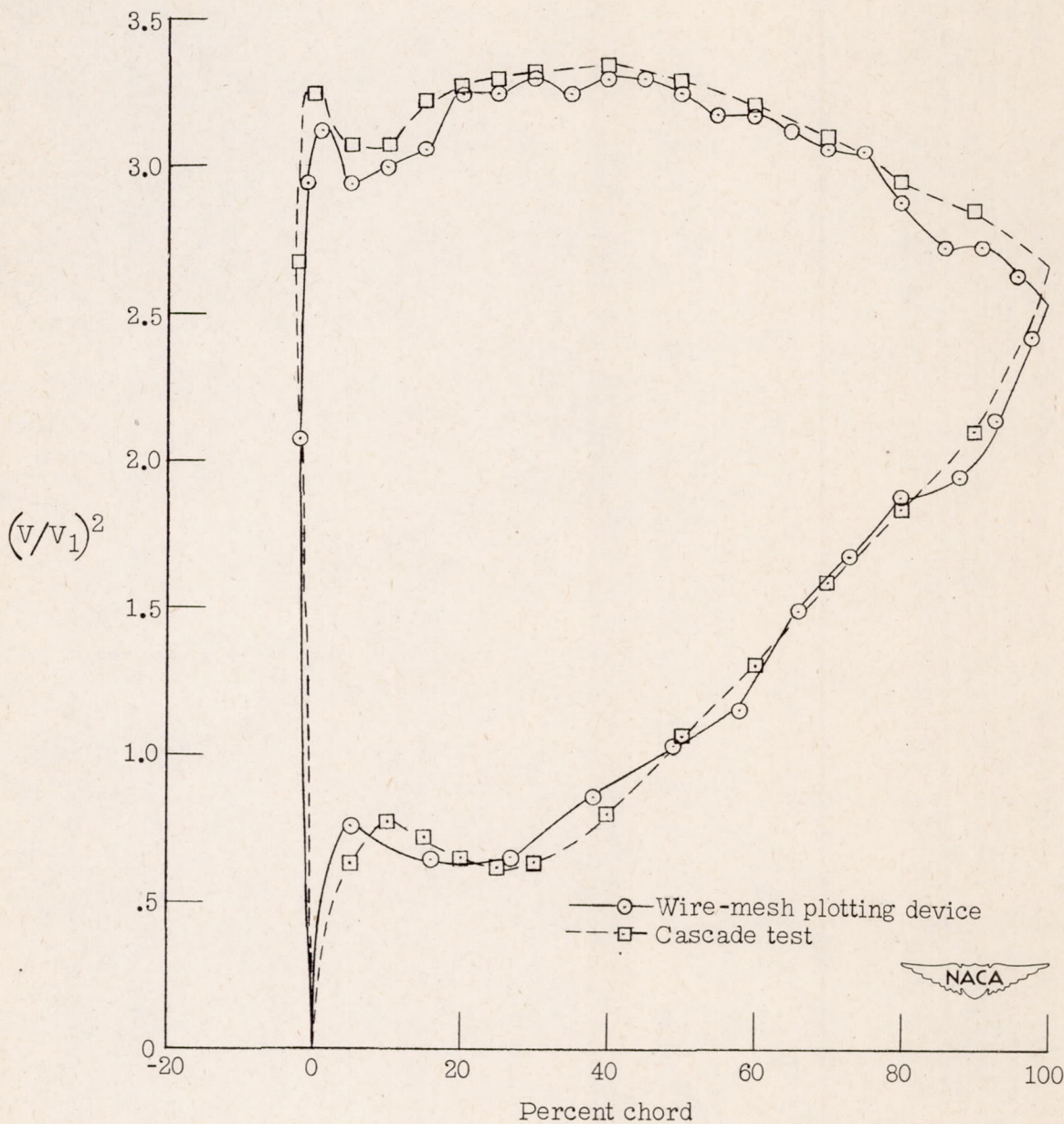
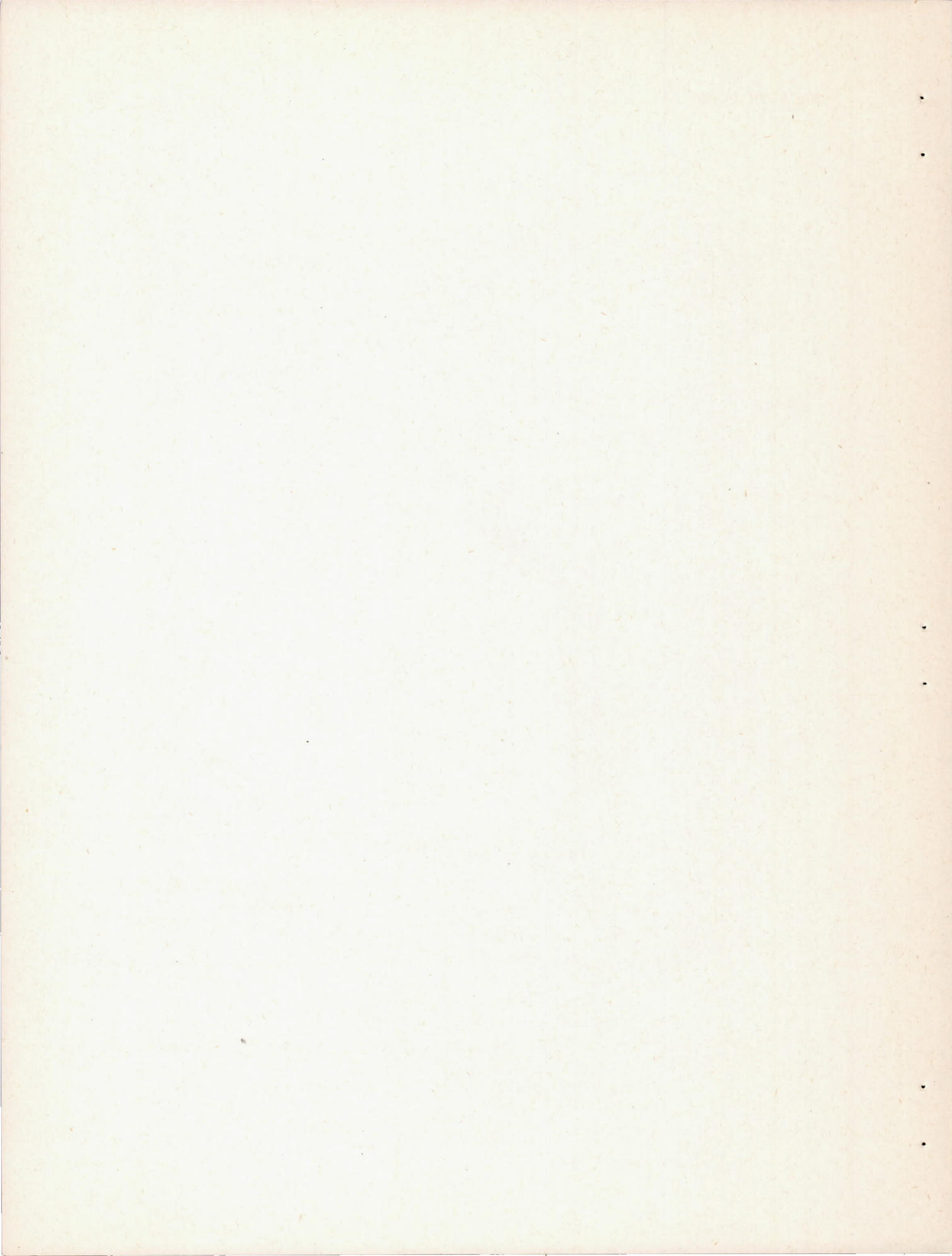


Figure 8.- Pressure distribution for blade II at 30° stagger and 1.8 solidity.







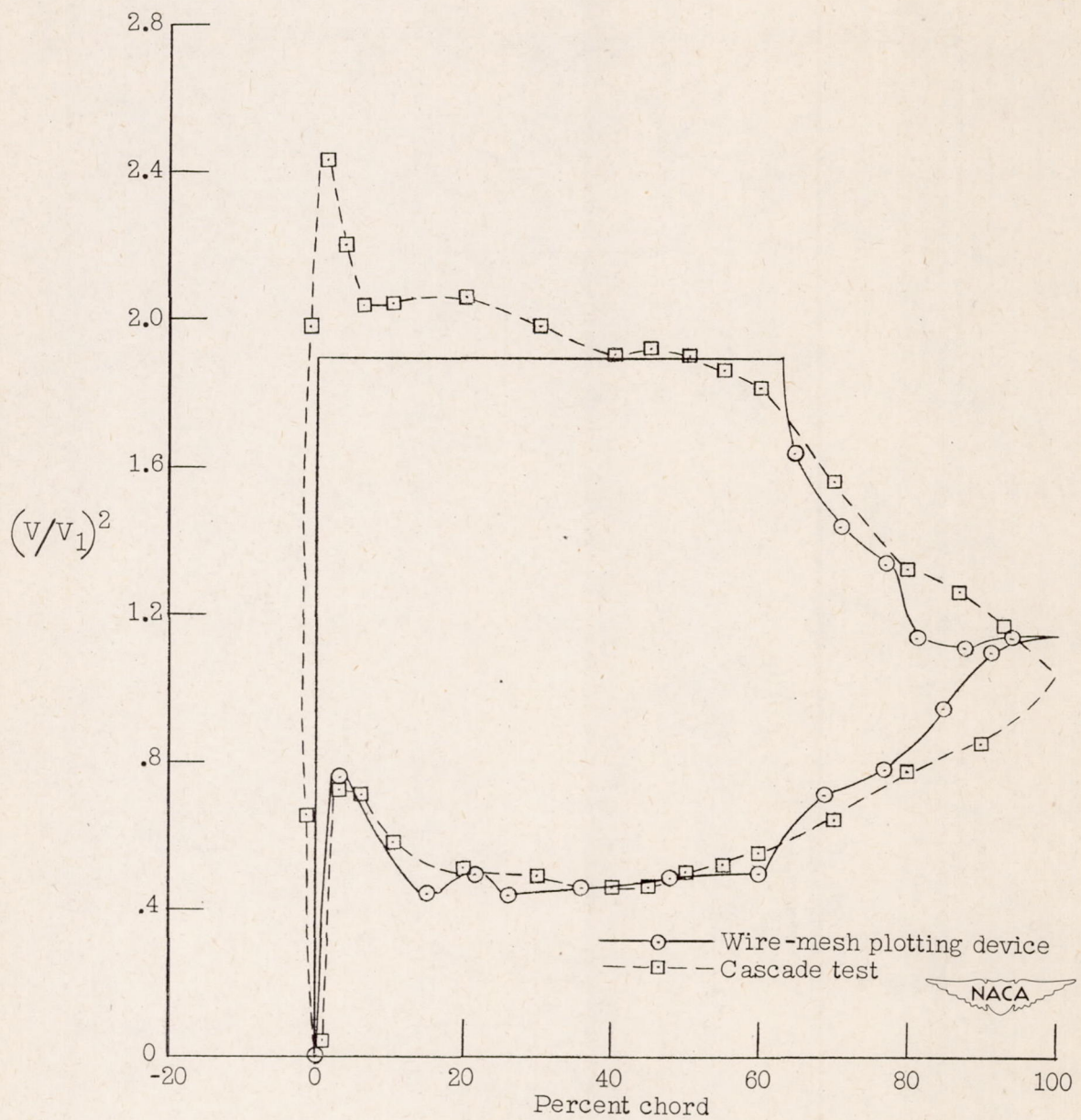


Figure 10.- Pressure distribution for blade III at 45° stagger and 1.8 solidity.

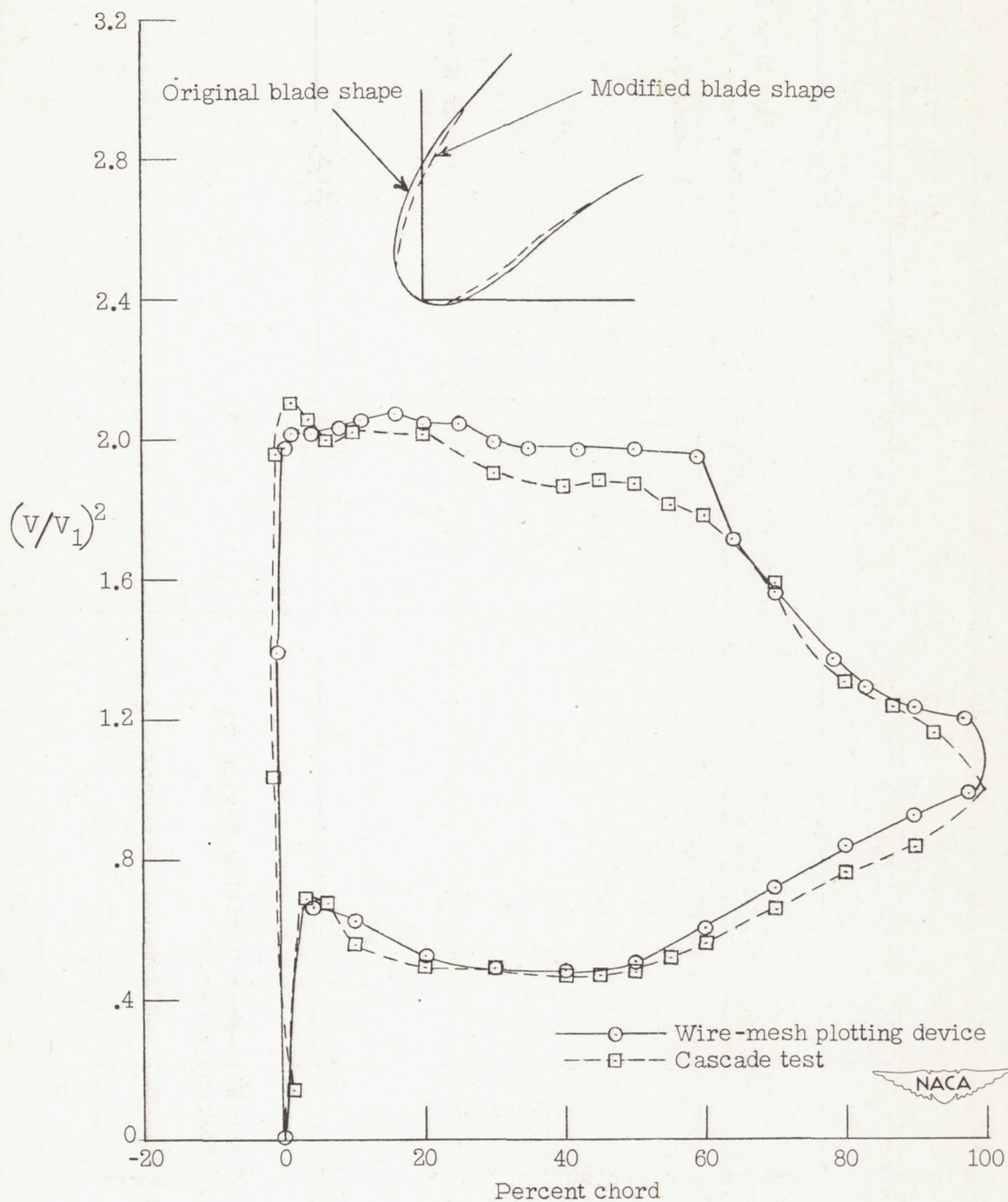


Figure 11.- Pressure distribution for blade III (modified) at  $45^\circ$  stagger and 1.8 solidity.